Microplastics and Nanoplastics

RESEARCH

Open Access

Vertical distribution and post-depositional translocation of microplastics in a Rhine floodplain soil

Pauline Seidel[1,2,3], Markus Rolf[3*], Anja Holzinger[4], Marie Gröbner[3,5], Svenja Riedesel[5,6], Hannes Laermanns[3], Heike Feldhaar[4], Christian Laforsch[7], Martin G. J. Loeder[7] and Christina Bogner[3*]

Abstract

Microplastics (MPs) are ubiquitous in the environment, but their vertical movement in undisturbed soils is poorly understood. This study investigates MP distribution and transport in one 110 cm soil profile from a Rhine River floodplain, Germany. Nine soil samples were analyzed for MP content, grain size distribution, bulk density, porosity, and organic carbon content. MPs (10 μm to 5 mm) were characterized by size, shape, and polymer type using ATR-FTIR and μFTIR. Biological activity was assessed through earthworm species identification and abundance, and sediment deposition was dated using optically stimulated luminescence (OSL). To our knowledge, this is one of the first studies to integrate detailed field observations with dating results to draw conclusions about the vertical displacement of microplastics. MPs were detected at all depths, with 81.3%–96.6% being 10–150 μm in size, predominantly fragments and spheres. Concentrations peaked at 790,497 particles kg^{-1} dry soil between 38 and 45 cm, where root- and earthworm-formed macropores facilitated transport. Below this depth, reduced porosity limited movement, favoring smaller MPs. OSL dating indicated sedimentation before the 1950s/60s below 20 cm, suggesting vertical transport of MPs. Therefore, we would advise to be careful using small MPs as stratigraphic markers for the Anthropocene. Although analysing just one soil profile, this study highlights the role of biological activity and soil structure in MP translocation and emphasizes the need to account for small MPs in floodplain studies to avoid underestimating their environmental presence.

Keywords Microplastic transport, OSL dating, FTIR spectroscopy, Bioturbation, Floodplain, Rhine river

*Correspondence:
Markus Rolf
markus.rolf@uni-koeln.de
Christina Bogner
christina.bogner@uni-koeln.de
Full list of author information is available at the end of the article

Graphical Abstract

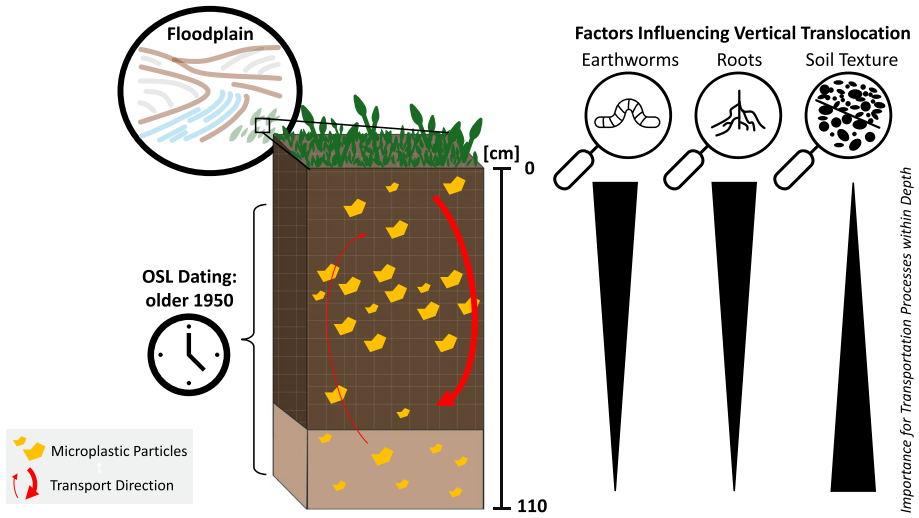

Introduction

With the onset of large-scale plastic production in the 1950 s and 1960 s, plastics began to enter the environment, notably through various human activities, including the discharge of wastewater, the use of sewage sludge in agriculture, littering, wind drift, and surface run-off [1–3]. Plastics in the environment appear either as larger macroplastics or smaller microplastics (MPs). In this study, we focus on MPs and adhere to the ISO definition, considering MPs as particles ranging from 1 to 5,000 µm in size [4].

MPs have been detected in all environmental compartments, from oceans [5] to Arctic ice [6] and even remote mountain regions [7]. In addition to ocean currents and atmospheric transport, rivers serve as major pathways for microplastic (MP) transport [8–11]. For example, in the river Rhine, concentrations of up to 1 g kg^{-1} dry sediment [12] or nearly 7 MP particles per m^3 of water [13] have been reported — values that are comparatively high in light of global freshwater concentrations, which range from 3.5 $\times 10^{-4}$ to 0.32 MP L^{-1} [14]. During floods, MPs carried by rivers can be deposited in the surrounding floodplains [15–18] together with sediments and organic material, building up the floodplains' fluvisols. This suggests that floodplains could serve as substantial – at least temporal – sinks for MPs of fluvial origin [19].

The growing scientific evidence indicates that once the MPs reached the soil, they could affect plants, soil biota, and soil properties [20, 21], raising concerns about food security and human health [8, 22, 23]. To date, most research has focused on MPs in the top 30 cm of a soil [24, 25], typically examining particles larger than 125 µm [7, 16, 19, 26]. Current assumptions suggest that MPs are transported primarily by large soil fauna such as earthworms and percolating water, with preferential flow paths such as large soil pores and biopores (e.g., earthworm burrows) facilitating their movement and the earthworms themselves acting as potential vectors [16, 17, 26–32].

Most MP vertical transport studies are conducted in soil column experiments under disturbed conditions without a soil structure and evaluating microplastic distribution [33–37]. Unstructured soils are rarely found in natural environments, and experiments based on them yield limited insights into microplastic transport under realistic soil conditions. Additionally, a significant knowledge gap exists regarding the behaviour and transport mechanisms of smaller MPs, particularly their distribution at greater soil depths and the conditions under which MPs of varying sizes, shapes and polymer types undergo vertical translocation within soils (e.g. [9, 16, 25, 38]). We analysed just one soil profile, but in depth with a large variety of methods. Collecting and analysing these data will help to understand whether, and under what conditions, MPs of varying sizes, shapes and polymer types are vertically translocated within soils.

To address these knowledge gaps, we studied the vertical distribution of MPs within one soil profile to analyse their possible vertical translocation after deposition. We address the research questions (i) whether MPs are vertically translocated in the investigated fluvisol soil profile following deposition, or whether they are co-deposited

with natural sediments only; and (ii) how possible vertical transport is related to soil and MP properties such as size, shape, and polymer type. Therefore, we collected nine soil samples from a 110 cm deep soil profile in a Rhine river floodplain and analyzed soil properties, biological activity by collecting earthworms, and the number of MPs in the soil. Finally, OSL dating was performed at five different soil depths to constrain the deposition ages of the floodplain sediments and to identify any potential post-depositional vertical transport of MPs within the soil profile.

Materials and methods

Study site

The studied floodplain is located in the north of the city of Cologne (Germany) at the left shore of the Lower Rhine river (Fig. 1). The area receives an annual precipitation of 805 mm and has a mean annual temperature of 9.8 °C, both peaking in summer [39]. The floodplain is a nature reserve covered by permanent grassland and its accessibility is limited to designated pathways [40]. Additionally, the floodplain is separated from built-up areas by a dike, so surface runoff from external sources can be excluded. The analysis of aerial photographs (1945; 1988–1994) showed no major changes in the land use [9], and we can exclude larger inputs of MPs through other processes than fluvial input. The groundwater level averages 34.92 m a.s.l. (above sea level) [41], while the site itself is situated at 37.65 m a.s.l. [9]. Hydrological simulations showed that the site was flooded two to three times a year on average [9], showing a pluvio-nival discharge regime [42, 43].

MPs in the studied floodplain are deposited primarily by the Rhine River [9, 18]. However, we cannot exclude additional atmospheric deposition. The study site lies in a depression between the Rhine River and a dike, which limits MP input from urban run-off and serves as a natural sink for materials transported by floodwaters [9].

Soil sampling

Soil sampling took place in August and September 2021. We prepared a soil profile with stainless steel non-painted spates and shovels (depth: 120 cm, width: 126 cm) and classified it following the World Reference Base Classification (WRB) [45, 46] (see Fig. 2A). Along with their description of the soil horizons, we classified the root abundances and the root diameters, both in 5 cm intervals. We took all soil samples directly from this profile using plastic-free tools, and stored them in precleaned glass jars with glass lids (Weck GmbH, 1500 ml). For MP analysis specifically, we took nine bulk samples, at the following depths with respect to soil horizon boundaries: 0–10 cm, 17–21 cm, 30–34 cm, 38–45 cm, 45–52 cm, 52–60 cm, 80–85 cm, 90–100 cm, 100–110 cm. Further, we collected blank samples to account for possible contamination with MPs in the field (cf. section Blank samples and contamination prevention). To determine soil physical and chemical properties, we took 17 soil samples in 5 to 10 cm intervals (max. 120 cm depth) as bulk samples from the whole width of the profile. For grain size

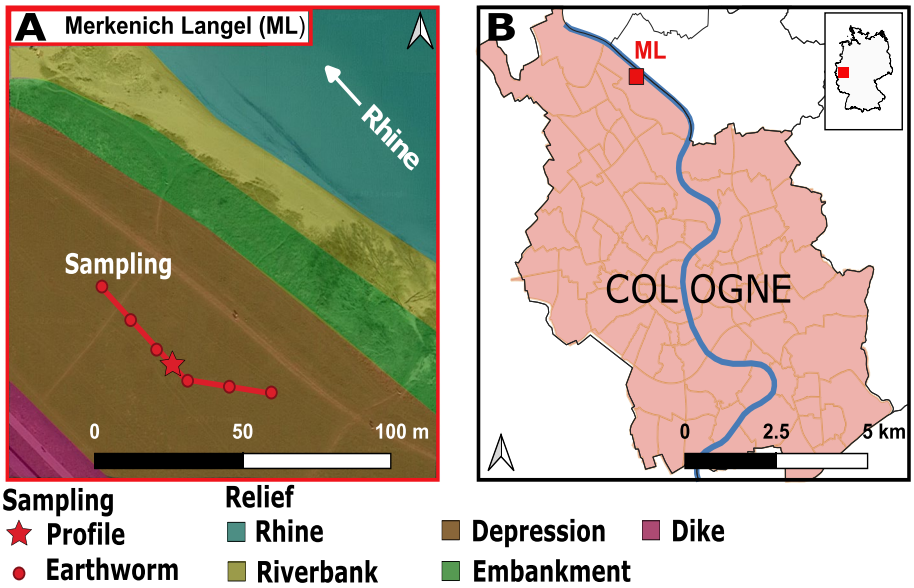

Fig. 1 Landform configuration of the study area (**A**). The sampling was done in one soil profile (red star) and nine earthworm sampling spots (red dots). Location of the study area (**B**). Spatial data was processed in QGIS (Version 3.28.3 Firenze) [44]

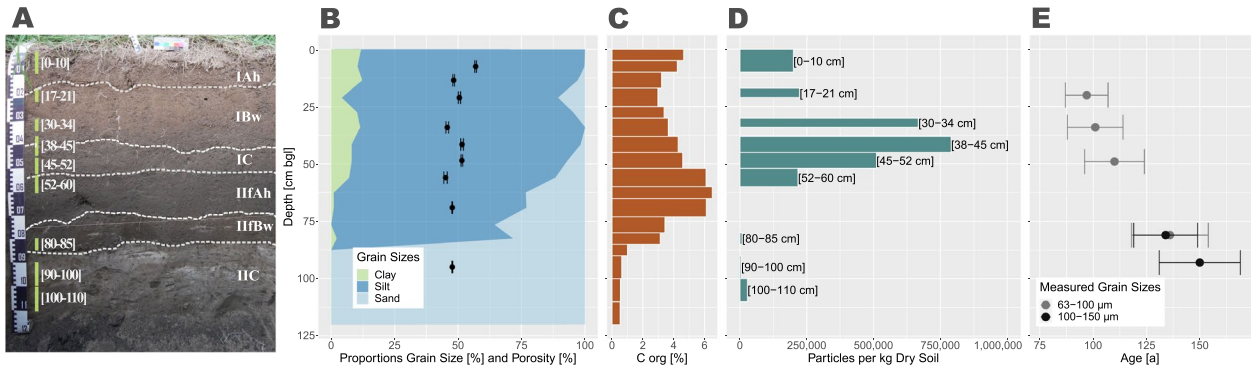

Fig. 2 **A** Image of the investigated profile showing soil classification, with abbreviations for soil horizons following the WRB classification system [46]. Grey dashed lines mark the boundaries between the horizons. The vertical green bars to the left of the sample names ([0–10] to [100–110]) indicate the depths in cm where the samples were collected. The uneven sampling intervals are due to the boundaries of the soil horizons. **B** Proportions of grain sizes, interpolated from individual measurement points. The position of the points on the *y*-axis corresponds to the mean depth of the bulk samples. The black dots represent measurements of soil porosity, along with their standard deviation. **C**, **D** Organic carbon content (C_{org}) and total number of MP particles per kg of dry soil across depth. Each bar represents one bulk sample, with the width corresponding to the sampling depth. Gaps between bars indicate where no samples were collected. **E** OSL ages for five different depths, with error bars showing the 1σ confidence interval

analysis, we dried the samples at 40 °C for 48 h, sieved them to < 2 mm, dissolved organic matter using hydrogen peroxide (H_2O_2, 15 %) and added 46 g L^{-1} sodium pyrophosphate ($Na_4P_2O_7$) to minimise aggregation. Three subsamples were measured per sample using a LS 13320 Beckmann Coulter^{TM} Laser Diffraction Particle Size Analyzer (116 channels, optical Fraunhofer model). Sample preparation for the other sedimentological analyses can be found in supplementary information, see Supplementary section 3.1. Additionally, we collected nine bulk density samples using stainless-steel corers (volume 100 cm^3) in 5 cm depth intervals (5–10 cm, 10–15 cm, 20–25 cm, 30–35 cm, 40–45 cm, 45–50 cm, 55–60 cm, 65–70 cm and 95–100 cm). For OSL dating, we collected five samples at 20 cm, 34 cm, 49 cm, 81 cm and 93 cm depth. Samples for dose rate determination were taken from each distinct sediment layer to account for possible variations in gamma dose rate delivered to the OSL samples.

Grain size measurements showed that silt is the dominant grain size throughout the entire profile, with 64.3 to 90.2 % per depth. Below 85 cm, the sediment consists solely of sand. Clay plays a subordinate role, making up 0 to 11.7 % (see also Fig. 2B). The dry bulk density was lowest in the topsoil sample (1.1 g cm^{-3}; 5 to 10 cm depth), highest in the deepest sandy horizons (1.4 g cm^{-3}; 95 to 100 cm depth) and fluctuated between values of 1.2 g cm^{-3} and 1.4 g cm^{-3} in between. Porosity was highest at 5 to 10 cm depth (56.9 ± 0.3) and lowest at 52 to 60 cm depth (45.1 ± 0.7), with values between 45.7 (± 0.5) and 51.5 (± 0.3) at the other soil depths. We classified the upper 10 cm and 52 to 60 cm as IAh and IIfAh horizons (WRB classification, [46], see also Fig. 2A) according to their colour and higher organic carbon contents. At the soil depths of 10–30 cm and 55–71 cm, we found weathered horizons and categorized them as IBw and IIfBw. The horizons inbetween (45 to 52 cm and below 85 cm) showed no further stratification and were classified as IC and IIC horizons.

Optically stimulated luminescence dating

Luminescence dating is used to date the last exposure of mineral grains (mainly quartz and feldspar) to daylight or heat. OSL uses the light-sensitive luminescence signal. For details on the methodological principle of luminescences dating, see Supplementary section 1.1.

We took five separate samples for OSL dating to analyse the depositional history of the floodplain sediments. We extracted sand-sized quartz grains for measurements as multiple subsamples by fixing grains on aluminium discs using silicone oil. These subsamples (aliquots) allow the assessment of any scatter in the data indicating insufficient resetting of the luminescence signal of the grains before deposition and were measured following the single aliquot regenerative dose protocol [47]. At least 24 of these aliquots were measured per sample.

Once a sufficiently large number of aliquots per sample had passed the necessary quality tests to validate them for dating, the dose carried by these aliquots was statistically evaluated using the unlogged minimum age model [48] to calculate a palaeodose for each sample. The palaeodose is then divided by the environmental dose rate, which is the sum of the external dose rate (calculated from the radionuclide concentrations in the sediment

surrounding the OSL sample) and cosmic dose rate (ionising radiation delivered to the sample from space). Further explanations regarding OSL, see Supplementary Material (section details of the luminescence dating).

Biological activity

We concentrated on the presence of earthworms as main contributors to both bioturbation, and thus creation of biopores, and biologically induced MP transport [49, 50], due to the absence of other large soil fauna of similar size. To determine the biological activity, soil sampling took place in September–October 2022 and April 2023, as earthworms are most active in autumn and spring [51]. We decided on two sampling periods to gain a more in-depth understanding of the diversity of earthworms. We took six soil monoliths during the first, and three more soil monoliths during the second sampling period, each monolith with a volume of 25 cm × 25 cm × 30 cm (W × L × D) and with a distance of 10 m between samples. We took the monoliths out of the soil at the same contour line as the soil profile (Fig. 1). All earthworms were manually extracted from the soil, and preserved in 80 % ethanol for subsequent species identification. We determined species abundance by counting the number of individuals per specie and identified adult earthworms to species level according to Sims and Gerard [51] using a Leica M165C stereomicroscope (Leica Microsystems, Wetzlar, Germany). We assigned every species to one of the three ecological categories (epigeic, anecic and endogeic) to draw conclusions about the depth of the inhabited soil and the movement patterns of the earthworms [51–53].

Extraction of microplastics

Microplastics > 500 μm

MP particles > 500 μm were extracted following the protocol by Möller et al. [54]. We freeze-dried the soil samples in glass containers covered with an ash-free paper filter (pore size: 2 μm) to disperse soil aggregates. After homogenisation, we divided each batch into 250 g subsamples and wet-sieved them in a stainless-steel sieving cascade (5 mm, 1 mm, 0.5 mm). Subsequently, we manually removed the visible organic material from each sieve and rinsed the potential MPs off onto the respective sieve. After sieving, we collected and separated the fine fraction (< 500 μm) in a cleaned glass jar. We covered the glass jar with an ash free paper filter (pore size: 10 μm) and dried the sample at 50°C. The remaining sample material of each larger size fraction (0.5 mm, 1 mm, 5 mm) was then sorted for putative MPs under a binocular stereo microscope (Motic, DM143) and photographed with a light microscope (Zeiss, axiolab 5). All putative MPs were stored in microcentrifuge tubes (Eppendorf, 1.5 ml) until the measurement with ATR-FTIR.

Microplastics < 500 μm

To extract MPs < 500 μm, we primarily followed the purification protocol by Möller et al. [54]: It consists of several density separations and enzymatic-oxidative digestion (Supplementary Fig. S2). The study by Rolf et al. [9], conducted at the same site, reported large amounts of MPs in the soil. Therefore, instead of using a 250 g subsample as suggested by Möller et al. [54], we used a 100 g subsample (dry weight) of the sieved fraction (< 0.5 mm), obtained through the cone-and-quarter-method. 50 g were used for the MP analysis and from the remaining 50 g subsample, we took 3 × 10 g subsamples to determine the remaining water content according to DIN EN 15934:2012-11 [55].

Density separation was performed using zinc chloride (ρ = 1.6 g cm^{-3}). A 50 g soil subsample was added to a straight-walled separation funnel and left to settle for 24 hours. After this period, the lower two-thirds containing the settled sediment were released, while the upper third of the liquid and material adhering to the funnel walls were retained, as they already contained a purified low-density fraction with MPs. Due to the high clay and silt content, the density separation had to be repeated with the settled sediments and prolonged to 24 hours. After the density separation, we conducted an enzymatic-oxidative digestion to remove the organic fraction in the sample [54] (see also Supplementary Fig. S2). Since the soil samples contained black carbon, we subsequently conducted another density separation with a calcium chloride solution (ρ = 1.2–1.4 g cm^{-3}), mainly following the protocol by Rolf et al. [9]. The particles separated into two layers: a floating, less dense layer depleted of black carbon; and a denser layer enriched with black carbon at the bottom. After separation, the samples were frozen at −20 °C to prevent beakers from breaking and the frozen layers were separated into two different glass beakers.

After thawing, we transferred both MP fractions onto separate stainless steel mesh discs (mesh size 5 μm, Rolf Körner GmbH). Since the filter cake was too thick to be measured via μFTIR directly, we divided the filters containing the MP-enriched fraction into eight parts, and those containing the black-carbon-enriched fraction into 64 parts using in-house designed side-cutting pliers. One of these eight or 64 parts, respectively, was then randomly selected and transferred onto analysis filters (aluminium oxide, mesh size 0.2 μm, Anodisc; Whatman GE Healthcare), depending on the amount of sampling material. This whole procedure resulted in six or seven sample carriers per soil sample.

Blank samples and contamination prevention

During the sampling process and preparation, we measured potential MP contamination with blank samples.

Subsequently, the number of MPs found in the blank samples was subtracted – MP shape-, size- and polymer type wise – from the data to produce the final MP results. Additionally, we took measures to avoid MP contamination during sampling and sample preparation. For more detailed information, we are referring to the Supplementary section 3.2.

Blank1 (B1) and Blank2 (B2), the two blank samples representing possible laboratory contamination, contained 824 and 192 MP particles, respectively. Blank3 (B3), representing possible laboratory and field contamination, contained 3,008 MP particles per kg. The particles in B1 were all fragments, made of 11 different polymers (ABS, EVAc, EVOH, PA, PBT, PE, PET, POM, PP, PS, Silicone) with sizes ranging from 11 to 113 µm. B2 consisted of PET fibers and fragments with sizes between 23 and 596 µm. B3 contained mainly fragments, secondarily also fibers and spheres made of seven different polymer types (ABS, PBT, PE, PET, POM, PP, PS) with sizes between 11 and 280 µm. Taking into account the weighing factors (section Microplastics < 500 µm and Supplementary section 3.2), we found a total of 3,508 particles per kg in our blank samples. As described above, the number of MPs found in the blanks were subtracted from the total number of MPs, and only blank corrected data are shown in this study.

FTIR measurements

Microplastics > 500 µm

First, we measured the length and width of each putative MP particle under a binocular microscope and recorded the shape (sphere, fibre, fragment). Then, we used an ATR-FTIR spectrometer (Bruker Alpha II) with platinum ATR and diamond ATR crystal to analyze all MP particles > 500 µm in a wave number range from 4000 to 400 cm^{-1}, 8 cm^{-1} resolution and an accumulation of 8 scans. We performed one background scan against the air before each series of measurement. For polymer identification, we used an in-house spectral polymer database [56].

Microplastics < 500 µm

For the smaller MPs, we measured each sample Anodisc filter by µFTIR (Lumos II, Bruker Optics GmbH & Co. KG, Ettlingen, Germany) in transition mode with a resolution of 8 cm^{-1} in a wave number range from 3600 to 1250 cm^{-1} without binning, resulting in a µ FTIR pixel size of 5.6 × 5.6 µm. The samples were measured with one scan, the background spectrum with 36 accumulated scans. We transformed the spectral data to an ENVI file using OPUS software (version 8.7, Bruker Optics GmbH & Co. KG, Ettlingen, Germany) and subsequently analysed the MPs with the Purency software (version 4.07, Purency GmbH) automatically. We classified the plastic particles with the 'Bayreuth Particle Finder' (version 3.04) – a random forest decision classifier that compares the measured spectra from µ FTIR with a database containing the 22 most common polymers types (ABS, CA, EVAc, EVOH, PA, PAN, PBT, PC, PE, PEEK, PET, PLA, PLA-PBAT, PMMA, POM, PP, PPSU, PS, PSU, PU, PVC, Silicone) [57]. We set all applicable thresholds to 0 to obtain raw data. The results of the automated classification and size measurement (widest dimension per particle) of each MP particle was checked by trained staff for QA/QC. Based on false-positive single hits in the chemical images, we adjusted the particle size when necessary. The shapes of the respective particles were added manually and for fibers, we individually measured their length and width. In the supplementary material, there is an example for microplastic particles identified on an analysis filter (Supplementary Fig. S6).

Data analysis

For data analysis, we used the R package evalPurency (version 1.2.4.9009) [58] to subtract the blank sample results (section Blank samples and contamination prevention) by size, shape, and polymer type from the particles recorded in each sample. We categorized MPs into the following size classes, focusing on small MPs due to their potential transport behaviour: > 10-20, > 20-50, > 50-100, > 100-150, > 150-300, > 300-500, > 500-1,000, > 1,000-5,000 µm. Finally, we used the shape classes fragments, spheres, and fibers (examples for each class, see Supplementary Fig. S8).

We used R Studio (version 2022.12.0+353) [59] under R (version 4.2.2 for Windows) [60] as well as the tidyverse package version 1.3.2 [61] for further processing and visualisation of MP data. We normalized the number of particles found during the analysis to 1 kg dry weight of soil. We used ChatGPT-3.5 and GPT-4o (OpenAI, 2025) to support grammar correction and improve language clarity during the drafting process. As none of the authors are native English speakers, this assistance helped ensure readability. All content was critically reviewed and revised by the authors to maintain scientific accuracy and integrity.

Results

Characteristics of the study site

Soil profile

The Rhine River transports about 2 Mt silt and clay each year, and the floodplains along the river are considered important sinks for those sediments [62]. This is confirmed by the soil particle size distribution: according to FAO guidelines [45, 46], the measured

texture is classified as silt and silty loam from 0 to 85 cm, and sand from 85 to 110 cm. The horizon boundary at 85 cm reflects alluvial loam horizon packages above and alluvial sands below [62, 63] (Fig. 2). According to the location and the soil particle size distribution, the site's predominant soil type is classified as fluvisol (WRB 2014) [46] with a silty loam texture [40]. This is associated with different ratios of pore volume and macropores (silt: 15 ± 10 %, sand: 30 %) in general [64].

Biological activity

The diameter of the roots varied with depth. In the upper 5 cm of the profile, roots of medium and fine diameter occurred (classification according to [45], section Soil sampling). While fine roots dominated the profile down to 40 cm, very fine roots were found from 45 to 90 cm. The root abundance in the upper 40 cm of the soil body can be classified as "common" and decreased constantly from 40 to 95 cm. Roots were also responsible for large macropores referred to as biopores. Below 95 cm, no roots were found.

In total, we identified ten species of earthworms in the 9 soil monoliths, with a total of 35 epigeic, 87 endogeic, and 10 anecic deep-burrowing earthworms. Epigeic earthworms, which are present and active in the upper 5 cm of the soil layer, were rare and consisted of the following species with their respective abundances, *Lumbricus rubellus*: 20, *Lumbricus castaneus*: 13, *Lumbricus festivus*: 1 and *Eisenia fetida*: 1. An even lower number was found for deep-burrowing anecic earthworms, namely *Lumbricus terrestris*: 8 and *Allolobophora longa*: 2. The soil depth between 5 and 30 cm, where endogeic earthworms were present, showed the highest level of biological activity across all samples. Endogeic earthworms consisted of *Allolobophora chlorotica*: 63, *Aporrectodea caliginosa*: 17 and *Allolobophora rosea*: 7, and are known to form widely branched and extensive subhorizontal burrow networks [65]. By burrowing as well as forming casts and refilling their burrows with compacted material, they are responsible for the formation of small (2–6 mm) as well as larger (> 6 mm) macropores also referred to as biopores [66], which were also visible at our study site (Supplementary Fig. S4).

OSL ages of sediments

OSL dating of coarse grain quartz extracted from five different soil samples revealed sediment deposition from 1852 until 1934 AD (1 σ) (Fig. 2E). The OSL ages are in stratigraphic order, with the oldest sample taken at a depth of 93 cm constraining the deposition of the distinctive sand layer to 1852-1890 AD. All other samples were collected within the alluvial sediments, with the sample at a depth of 81 cm constraining the start of its deposition to the late 19th century AD (Supplementary Table S3).

Due to the variation in grain sizes throughout the profile, different sand-sized fractions were used for OSL dating throughout the profile. Whilst for the OSL sample collected in the IIC horizon (depth: 93 cm) no material finer than 100 μm was available, a grain size of 100–150 μm was used for dating. In contrast, the samples collected from the alluvial part of the profile yielded finer material, thus necessitating a change in grain size for OSL dating. For the upper four samples, we therefore used quartz in the range of 63–100 μm for dating. The sample in 81 cm depth, however, yielded material within in both fractions, allowing for a comparison of both grain size fractions. The two fractions dated for this sample yielded consistent results, with the fraction 100–150 μm yielding an age of 134 ± 15 years, and the 63–100 μm yielding an age of 136 ± 18 years. These findings support the above described OSL chronology of the entire profile (Supplementary Table S3).

Microplastic characteristics and depth distribution

We detected MPs and coarse plastic particles in all investigated samples, ranging from 10 µm up to approx. 23,500 µm in size. 84 particles per kg were > 5,000 µm in size, mainly fibers, and therefore were excluded from further calculations according to the size definition of MPs. Of all analysed MPs, 51.4 % were fragments, 47.4 % were spheres and 1.2 % were fibers. The vast majority of MP particles were made of PS (62.4 %), followed by PVC (13.4 %), PE (8.3 %), PP (4.4 %) and PA (3.0 %) (Supplementary Fig. S8). The other polymer types found (n = 13; namely ABS, EVAc, EVOH, PAN, PBT, PC, PET, PLA-PBAT, PMMA, POM, PSU, PU, Silicone) made up less than 3 % each.

Starting from the uppermost sample (0 to 10 cm depth), the concentration of MP particles per kg increased within the profile to its maximum (790,497 particles kg^{-1}) at a depth between 38 and 45 cm (Fig. 2D). Below 85 cm, the abundance of MP decreased to its minimum with 4,923 particles kg^{-1} at a depth of 90 to 100 cm.

Two groups of sizes became evident: a majority (87.5 %) of particles per kg were in the size range of 10 to 150 µm, accounting for 81.3 to 96.6 % of MPs in individual samples (Fig. 3B). The minority of particles fell in the larger size classes > 150 µm, comprising 3.5 % to 18.8 % of individual samples. The size distribution varied with soil depth, as samples from 0 to 85 cm differed from those at 90 to 110 cm, with deeper samples containing a higher proportion of smaller particles (10 to 50µm).

The distribution of MP shapes across depth (Fig. 3C) showed that fragments dominated throughout the

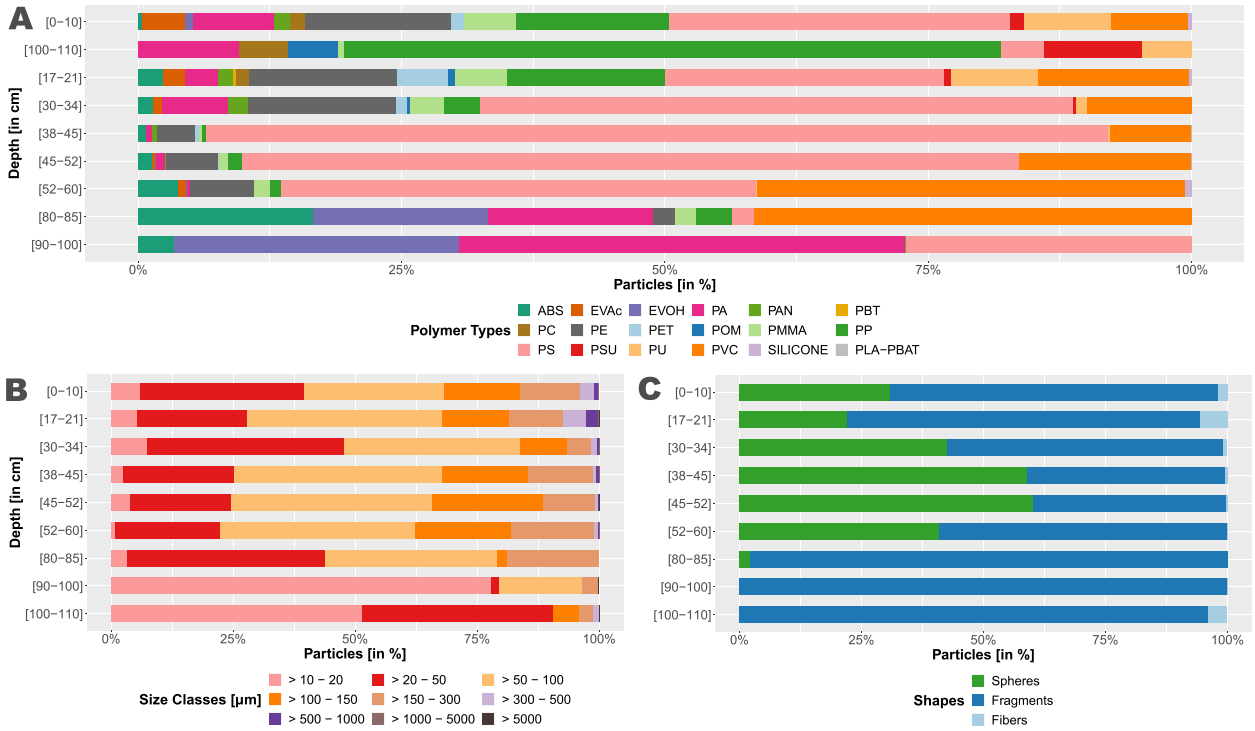

Fig. 3 Composition of MP particles size for each sample, arranged in increasing depth from top to bottom and categorized into merged **A** polymer types, **B** size classes and **C** shapes

entire profile (56.4 % to 100.0 % in individual samples) except for two samples (38 to 45 cm and 45 to 52 cm). Here, spheres dominated, making up around 60 % in each sample. Between 52 and 85 cm depth, the abundance of spheres decreased from 41 % to 2 %. Below this depth, no spheres were found. The majority of spheres coincided with the depths of the highest MP numbers. Fibers play a minor role throughout the profile, varying between 0 to 5.6 % in individual samples.

When examining the distribution of polymer types with depth, no clear patterns were observed (Fig. 3A). We expected patterns according to the polymer densities, e.g. that lighter polymers stay in the uppermost layers according to their lower density; and denser, heavier particles migrate deeper into the depth profile. The results do not confirm this pattern, as denser polymers like PET, PBT and PVC did not occur in the deepest samples, nor did lighter polymers like EVAc or silicones. At the same time, lighter polymers like ABS, PE or PP were not restricted to the uppermost sedimentary layers. However, the heterogeneity of polymer types decreases with increasing depth, meaning that a greater variety was found in the upper samples.

Discussion

Abundance and characteristics of microplastics

Abundance of microplastics

Within the soil profile, we found on average 294,709 ± 293,410 MP kg^{-1} dry soil in each depth. The maximum abundance of MP in this study, with almost 800,000 particles kg^{-1} dry soil, exceeded the numbers reported in the literature for floodplains by far. Other studies in floodplains found much smaller numbers. For example, Scheurer and Bigalke [7] (125–5000 µm; sampling depth 5 cm) detected a maximum of 593 particles kg^{-1}, Jiao et al. [67] (60–2500 µm; sampling depth 5 cm) 495 particles kg^{-1} and Lechthaler et al. [19] (500–5000 µm; sampling depth 110 cm) 47.9 particles kg^{-1}. Even in agricultural soils, known for their high MP content [25, 68], studies found fewer MPs, e.g. 252.7 particles kg^{-1} for agriculturally used floodplains in China [69] (<100–5000 µm; sampling depth 80 cm).

The observed differences are most likely due to the fact that most studies focusing on MPs in floodplain sediments (e.g. [16, 26, 70]) primarily analysed larger MPs typically starting at around 100 µm in size, with the exception of Rolf et al. [9, 18]. In contrast, in our study, small MPs (<150 µm) accounted for approximately 81% to 97% of the total MPs in individual samples, suggesting that many previous studies may have underestimated MP numbers.

Another factor contributing to the difference in particle counts is the variation in analytical methods for detecting MPs. This study used µFTIR, whereas some other studies in floodplains relied on visual extraction under a microscope (e.g. [16, 19]). Even studies using µFTIR differ. For example, Rolf et al. [9] examined the MPs at the same site at 20 cm depth in the 11–5000 µm range and found up to 85,000 particles per kg dry soil. Although we analysed MPs in a similar size range, we found up to ten times more particles than Rolf et al. [9]. This might be partly due to natural variability. However, although both studies followed the same sampling and sample preparation protocols, they used different µFTIR instruments: Rolf et al. [9] employed a Hyperion 3000 (Bruker), while this study used the LUMOS II µFTIR (Bruker). The latter has a shorter path between the infrared beam and the sample, resulting in less total absorption and more precise spectra.

The abundances of MPs were lower below 52 cm compared to the upper sections of the profile, consistent with the trend observed in most studies, which reported decreasing MP concentrations with increasing soil depth (e.g. [26, 71, 72]). In this study, lower MP abundances from 52 cm downwards might be caused by the lower root densities in these lower soil layers (52 to 100 cm) and lower abundances of anecic earthworms (10 individuals). This results in smaller biopores and thus less vertical transport of MPs via preferential flow of water and biota.

Sizes, shapes, and polymer types of microplastics

We can distinguish the samples in 0 to 85 cm from those in 90 to 110 cm depth, as there is an increase in smaller particles (> 10 to 50 µm) in those deepest samples (Fig. 3B), indicating a size-dependent depth distribution. In general, small MPs dominated in the analysed samples in our study (87.5 %; size range: > 10 to 150 µm). Zhou et al. [73] and Rolf et al. [9] reported comparable results, where particles < 100 µm [< 150 µm] accounted for 81.7 % [75.0 %] of detected MPs. Rolf et al. [18], who sampled at the same location, found that only 49.0–53.6% of MPs were within the 20–100 µm size range. This may be attributed to their shallower sampling depth (maximum 20 cm) and to the fact that they only focussed on four different polymer types (PS, PE, PP, PET).

The dominance of fragments in 7 out of 9 samples (56.4 up to 100.0 % in individual samples) is consistent with other floodplain studies (e.g. [9, 18, 70]), regardless of whether those studies distinguished between MP films and fragments (e.g. 82.3 % in Lechthaler et al. [19], 73.8 % in Weber et al. [16] and 84.1 % in Weber et al. [17]).

We found that 77 % [92 %] of all spheres, which are typical examples of primary microplastics, were smaller than 100 µm [150 µm]. The majority of the spheres (over 90 %) were made of PS. Rolf et al. [9], who sampled at the same site, also detected PS spheres, with 70 % of their spheres being smaller than 100 µm. Furthermore, Rolf et al. [18] discovered polymer spheres 20 km upstream in the floodplains of the Rhine River. Also Mani et al. [74] found spheres in the water of the Rhine river, with 70 % of them made of PS. They sampled from Basel (Switzerland) to Rotterdam (Netherlands), finding one of the highest abundances of spheres close to the city of Leverkusen (Germany) that is nearby the site studied here. Furthermore, this suggests that the MPs in the studied fluvisol were deposited by the flooding of the Rhine river.

The shares of polymer types vary largely between studies in floodplains, however, PE and PP often dominate (cf. [7, 19, 70]). Exceptions are this study and the study by Rolf et al. [9] where PS prevail. This indicates that the primary MP sources might differ between studies, leading to different polymer distributions. The most abundant polymer types identified in this study align with the globally and European-wide most produced polymers in 2021—PP, PE, and PVC, primarily used as single-use plastics—with PS ranking as the fourth most produced polymer in Europe [75].

Relationship between vertical transport and MP characteristics

Microplastics can be transported vertically by water and through bioturbation [8, 16, 76]. In particular, macrofauna like earthworms facilitate the transport of MPs into and within soils (e.g. [29, 50, 77]). Earthworms can ingest MPs [78], incorporate them into burrows, and transport them on their skin [28, 29, 50, 77]. The study of Huerta Lwanga et al. [29] indicated that preferentially smaller MPs ($\leq$ 50 µm) can be moved by earthworms, although Rillig et al. [50] showed that also larger MPs (up to 2800 µm) can be displaced vertically.

We found MPs at all depths down to 110 cm. The vertical transport of MPs in our study is particularly affected by their size, with macropores playing a key role in MP displacement. The soil was primarily silty up to 85 cm and sandy below. This corresponds to theoretical diameters of texture-based macropores ranging

from 10 to over 50 μm, which account for approximately 15 ± 10% of the total pore volume in silty horizons and up to 30% in sandy horizons [64].

In addition to these texture-based pores, we found macropores formed by roots and earthworms throughout the soil profile (see Supplementary Fig. S4), which can be substantially larger. According to the presence of anecic earthworms (10 individuals) in our investigated profile and recent burrows down to 70 cm with diameters of up to 5 mm (Supplementary Fig. S4), MPs might have been transported downward by earthworms or preferential flow of water. Sampling based on hand-sorting potentially leads to an underestimation of anecic earthworms due to their flight instinct triggered by disturbances [79, 80]. The high abundance of MPs in 30 to 52 cm depth corresponds to the high abundance of endogeic earthworms (87 individuals) and their burrows that we detected in 5 to 50 cm depth (section Biological activity). The roots also form larger pores and act as preferential pathways for the transport of MPs by water. The high porosity values between 38 and 52 cm indicate the presence of these macropores, presumably formed by earthworms and roots, and we found a maximum of MPs there. Below this depth, the porosity decreased and MP transport downward is reduced but not stopped. In the deeper soil, some macropores were still present and can serve as transport pathways. However, there, the transport might be predominantly through textural macropores, which could explain the dominance of smaller microplastics (Fig. 3B).

In samples below 80 cm depth, we mainly found particles < 20 μm, which indicates a larger mobility of small MPs and agrees well with previous studies (cf. [16, 17, 32, 69, 81]). In addition, we analysed Spearman correlations between MP abundances within defined size classes and soil depth (Supplementary Fig. S7). For smaller MPs (< 300 μm), the depth distribution is non-linear, with a peak at 32 cm that coincides with a change in porosity. However, correlations with depth remain non-significant. In contrast, larger MPs (> 300μm) show more linear depth distributions with significant correlations. These patterns reflect different transport mechanisms: larger MPs are primarily transported through large, connected, and relatively rare pores, while smaller MPs can move through both large and small pores. As a result, their distribution more closely mirrors the measured variations in soil porosity.

The majority of spheres occurred at depths with the highest MP abundances. Larger spheres > 500 μm were restricted to 17 to 73 cm depth, and smaller spheres < 500 μm have reached a maximum depth of 85 cm. In addition, we have found few fibres in depths of 100 to 110 cm. The fibres may have been transported in those depths due to their high conformability and flexibility, or moved by soil fauna. These findings on the distribution of spheres and fibres within depth contradict the theory of [72] that spheres could be the most displaceable particles by shape, as they are most similar to natural soil particles. According to the distribution of spheres and fibres, we tend to assume a more size- than shape-dependent transport of MPs.

The role of polymer density has been considered as a key factor in microplastic transport through porous media such as soils [82, 83]. In particular, in experiments on disturbed columns without soil structure, they found low-density polymers to be more mobile and penetrate deeper into the columns than high-density polymers [31, 82]. However, we found denser (POM: 1.41 g cm^{-3}, PMMA: 1.18 g cm^{-3}, PA: approx. 1.15 g cm^{-3}, PU: 1.0–1.25 g cm^{-3}) and less dense microplastic particles (PP: approx. 0.91 g cm^{-3}, PE: approx. 0.93–0.97 g cm^{-3}) together in the same soil depth of 100–110 cm. This polymer-independent pattern occurs throughout the profile and can also be found in other environmental data from soil cores and profiles [16, 84]. Those patterns can be explained by the presence of large stable biopores that accelerate water flow through soil to deeper soil horizons, in particular, anecic earthworms burrows can last for months and years (diameter up to 5 mm) [85–87].

As a general pattern, we observed that the composition in terms of MPs size, shape and polymer type decreased across depth and varied less in their size and shape composition. Furthermore, no specific polymer type, size, or shape was exclusively found in either the upper or lower samples (e.g., there was no distinct layer of PE particles limited to depths above 20 cm). These findings support the hypothesis that MPs in the lower samples emanate from the samples above, meaning that they were transported downward.

Because our study is observational, we cannot distinguish between MP transport by bioturbation and MP transport via preferential flow of water. Similarly, we cannot differentiate about the size or shape of MPs transported by earthworms versus those transported by water. Thus, the observed vertical distribution of MPs in the studied profile is probably the result of both processes.

We combined multiple methods to study the vertical transport of MPs, gathering data on soil properties, biological activity, MP distribution and characteristics, and soil age. Although limited to a single profile, which constrains statistical analysis, this comprehensive dataset provides a coherent view of the potential mechanisms driving MP vertical displacement in soil and enables us to differentiate deposition from vertical translocation in the next section.

Disentangling deposition and vertical transport

The production of large polymer quantities started in the 1950s/1960s [88]. Since then, MPs may have entered the environment. The OSL dating results for this study's profile suggest sedimentation ages older than 1950s/1960s throughout the profile, implying that all MPs below 20 cm depth are transported within the profile. This means that 84.2 % of all found MPs (approx. 2.3 million MPs) have been vertically transported. OSL ages with overlapping error bars (i.e. indicating possible similar ages), especially towards the top of the soil profile, may either indicate rapid sedimentation due to recurring flooding of the Rhine River, or bioturbation, but limited locally to the top part of the profile. The presence of earthworms is a clear indicator for bioturbation. The OSL ages, the presence of earthworms and biopores suggest that the MP particles found in larger depths in the studied profile have been vertically displaced and not co-deposited with sediments.

Floodplains can act as sedimentation and retention areas, serving as sinks for sediments and MPs that systematically accumulate during flood events, provided there are no system disturbances [19, 26]. With the global increase in plastic production from the 1950 s and 1960 s and their simultaneous release into the environment, macro- and microplastic particles have been discussed as stratigraphical or anthropogenic markers in (floodplain) soils [17, 19, 89]. However, our study shows that this approach is not applicable to the investigated site, and possibly not to natural soils in general. Our results indicate that the majority of MPs are transported within the soil by bioturbation and water, as supported by OSL ages. The substantial increase in MP abundance between 38 and 45 cm depth is probably due to soil parameters, such as soil texture and bulk density and abundance of biopores, which affect the vertical transport. The sediments at this depth were deposited approximately in the 1930 s, before the mass production of plastics started. Furthermore, we found MPs at depths between 90 and 100 cm and the corresponding OSL sample at 93 cm depth dates back to the years 1852–1890, which is older than the invention of plastics itself. Therefore, the use of MPs as stratigraphical or anthropogenic marker should be carefully considered as other studies found similar patterns in limnic and other fluvial systems [72, 84]. However, it should be discussed if an abrupt increase in large MPs (> 2 mm, as suggested in Weber and Lechthaler [89]) in soils might mark the onset of the Anthropocene, due to their poor translocatability.

While our findings indicate vertical transport of MPs, and particularly smaller MPs particles, it is important to note that our study is based on a single soil profile without technical replication. This was primarily due to the considerable effort required for preparing soil samples deriving from actual fieldwork for analysis using particle-counting techniques such as μFTIR. Given the limited number of MP samples, the application of robust statistical methods remains constrained.

Conclusions

Based on these findings, we conclude that the vertical transport of MPs is strongly influenced by their size, the abundance of large soil pores and bioturbation. Smaller particles may be more easily transported downwards, and the shape and polymer type (density) of MPs seems to play a minor role. Because small MP can be transported deeply to older soil horizons, this should be considered before using them as stratigraphic or anthropogenic markers. Further research should analyse more soil profiles to assess MP abundances and characteristics in greater detail, as this study provides only initial insights into vertical transport based on the analysis of a single profile. While the majority of previous studies have predominantly focused on MP contamination in topsoils, our findings show that MP research should also take greater depths of soil profiles into account, to comprehensively assess the vertical distribution and long-term environmental fate of MPs in terrestrial ecosystems. We recommend following an interdisciplinary approach, combining state-of-the-art spectroscopic methods (like Raman and μFTIR) that allow for reliable data in the range of smaller MPs, dating and sedimentological methods, to enhance the understanding of MP behaviour in the soil environment, which could also contribute to a size-specific use of micro- and macroplastics as stratigraphic or anthropogenic markers.

Supplementary Information

The online version contains supplementary material available at https://doi.org/10.1186/s43591-025-00142-9.

Additional file 1. Additional figures, tables, and details on soil analyses, blank samples as well as OSL dating

Acknowledgements

The authors thank Ursula Wilczek, Julia Möller, Eva Cseperke Vizsolyi, Heghnar Martirosyan, Hannah Ganzleben and student assistants for their help during the entire laboratory process. Florian Rampp supported the determination of the earth- worms. Julia Horn analysed soil physico-chemical properties. Florian Steininger has substantially supported the field work. Marvin Kiene supported the μ-FPA-FTIR data analysis. Mirko Engelmann measured the ATR-FTIR spectra. We would like to thank Anja Zander (University of Cologne) for high-resolution gamma-spectrometry as well as Christopher-Bastian Roettig and Tony Reimann for insightful discussions of the results.

Authors'contributions

Conceptualization: CB, MGJL, HL and MR; Investigation: MR and HL (field work), PS and MR (prepared soil samples for FTIR analyzes), PS and MGJL (analyzed

μ-FPA-FTIR spectra), MG and SR (provided and analyzed OSL data), AH and HF (provided and analyzed earthworms' data); Visualization: PS and MR; Writing – Original Draft: PS, MR, SR, HL and CB; Writing – Review and Editing: all authors; Supervision: CB, MGJL, CL, HL and MR; Project administration and Funding acquisition: CB, MGJL and CL.

Funding
Open Access funding enabled and organized by Projekt DEAL. This study was funded by the Deutsche Forschungsgemeinschaft (DFG, German Research Foundation) – Project Number 391977956 – SFB 1357, and by the Funds for Student Research (Technical University Dresden).

Data availability
Data and code are published on ZENODO (https://doi.org/10.5281/zenodo.16792389). Raw spectra can be obtained from the authors upon reasonable request.

Declarations

Competing interests
The authors declare no competing interests.

Author details
[1]Heisenberg Chair of Physical Geography with Focus on Paleoenvironmental Research, Institute of Geography, Technical University of Dresden, Helmholtzstraße 10, Dresden 01069, Saxony, Germany. [2]Faculty of Agriculture, Environment and Chemistry, University of Applied Sciences Dresden, Friedrich-List-Platz 1, Dresden 01069, Saxony, Germany. [3]Ecosystem Research, Institute of Geography, Faculty of Mathematics and Natural Sciences, University of Cologne, Zülpicher Straße 45, Cologne 50674, North Rhine-Westphalia, Germany. [4]Animal Population Ecology, Animal Ecology I, BayCEER, University of Bayreuth, Universitätsstr. 30, Bayreuth 95440, Bavaria, Germany. [5]Geomorphology & Geochronology, Institute of Geography, Faculty of Mathematics and Natural Sciences, University of Cologne, Zülpicher Straße 45, Cologne 50674, North Rhine-Westphalia, Germany. [6]Luminescence Physics and Technologies, Department of Physics, Technical University of Denmark, Frederiksborgvej 399, Roskilde 4000, Sjælland, Denmark. [7]Animal Ecology I, BayCEER, University of Bayreuth, Universitätsstr. 30, Bayreuth 95440, Bavaria, Germany.

Received: 27 May 2025 Accepted: 1 August 2025
Published online: 13 August 2025

References

1. Geyer R, Jambeck JR, Law KL. Production, use, and fate of all plastics ever made. Sci Adv. 2017;3(7): e1700782. https://doi.org/10.1126/sciadv.1700782.
2. Alimi OS, Farner Budarz J, Hernandez LM, Tufenkji N. Microplastics and nanoplastics in aquatic environments: aggregation, deposition, and enhanced contaminant transport. Environ Sci Technol. 2018;52(4):1704–24. https://doi.org/10.1021/acs.est.7b05559.
3. Bläsing M, Amelung W. Plastics in soil: analytical methods and possible sources. Sci Total Environ. 2018;612:422–35. https://doi.org/10.1016/j.scitotenv.2017.08.086.
4. International Organization for Standardization. ISO/TR 21960:2020(en) Plastics — Environmental aspects — State of knowledge and methodologies. 2020. https://www.iso.org/obp/ui/#iso:std:iso:tr:21960:ed-1:v1:en. Accessed 27 Oct 2022.
5. Thompson RC, Olsen Y, Mitchell RP, Davis A, Rowland SJ, John AWG, et al. Lost at sea: where is all the plastic? Science. 2004;304(5672):838. https://doi.org/10.1126/science.1094559.
6. Bergmann M, Mützel S, Primpke S, Tekman MB, Trachsel J, Gerdts G. White and wonderful? Microplastics prevail in snow from the Alps to the Arctic. Sci Adv. 2019;5(8): eaax1157. https://doi.org/10.1126/sciadv.aax1157.
7. Scheurer M, Bigalke M. Microplastics in Swiss floodplain soils. Environ Sci Technol. 2018;52(6):3591–8. https://doi.org/10.1021/acs.est.7b06003.
8. Petersen F, Hubbart JA. The occurrence and transport of microplastics: the state of the science. Sci Total Environ. 2021;758: 143936. https://doi.org/10.1016/j.scitotenv.2020.143936.
9. Rolf M, Laermanns H, Kienzler L, Pohl C, Möller JN, Laforsch C, et al. Flooding frequency and floodplain topography determine abundance of microplastics in an alluvial Rhine soil. Sci Total Environ. 2022;836: 155141. https://doi.org/10.1016/j.scitotenv.2022.155141.
10. Kurzweg L. Microplastic analysis in sediments of the Elbe River by electrostatic separation and differential scanning calorimetry. Sci Total Environ. 2024;930(172514). https://doi.org/10.1016/j.scitotenv.2024.172514.
11. Stratmann CN, Dris R, Gasperi J, Buschman FA, Markus AA, Guerin S, et al. Monitoring microplastics in the Seine River in the Greater Paris area. Front Earth Sci. 2024;12: 1386547. https://doi.org/10.3389/feart.2024.1386547.
12. Klein S, Worch E, Knepper TP. Occurrence and spatial distribution of microplastics in river shore sediments of the Rhine-Main area in Germany. Environ Sci Technol. 2015;49(10):6070–6. https://doi.org/10.1021/acs.est.5b00492.
13. Mani T, Burkhardt-Holm P. Seasonal microplastics variation in nival and pluvial stretches of the Rhine River - from the Swiss catchment towards the North Sea. Sci Total Environ. 2020;707: 135579. https://doi.org/10.1016/j.scitotenv.2019.135579.
14. Horton AA, Walton A, Spurgeon DJ, Lahive E, Svendsen C. Microplastics in freshwater and terrestrial environments: evaluating the current understanding to identify the knowledge gaps and future research priorities. Sci Total Environ. 2017;586:127–41. https://doi.org/10.1016/j.scitotenv.2017.01.190.
15. Helcoski R, Yonkos LT, Sanchez A, Baldwin AH. Wetland soil microplastics are negatively related to vegetation cover and stem density. Environ Pollut. 2020;256: 113391. https://doi.org/10.1016/j.envpol.2019.113391.
16. Weber CJ, Opp C, Prume JA, Koch M, Andersen TJ, Chifflard P. Deposition and in-situ translocation of microplastics in floodplain soils. Sci Total Environ. 2022:152039. https://doi.org/10.1016/j.scitotenv.2021.152039.
17. Weber CJ, Opp C, Prume JA, Koch M, Chifflard P. Meso- and microplastic distribution and spatial connections to metal contaminations in highly cultivated and urbanised floodplain soilscapes - a case study from the Nidda River (Germany). Microplastics Nanoplastics. 2022;2(1):25. https://doi.org/10.1186/s43591-022-00044-0.
18. Rolf M, Laermanns H, Horn J, Kienzler L, Pohl C, Dierkes G, et al. Multi-method analysis of microplastic distribution by flood frequency and local topography in Rhine floodplains. Sci Total Environ. 2024;927: 171927. https://doi.org/10.1016/j.scitotenv.2024.171927.
19. Lechthaler S, Esser V, Schüttrumpf H, Stauch G. Why analysing microplastics in floodplains matters: application in a sedimentary context. Environ Sci Process Impacts. 2021;23(1):117–31. https://doi.org/10.1039/D0EM00431F.
20. de Souza Machado AA, Lau CW, Kloas W, Bergmann J, Bachelier JB, Faltin E, et al. Microplastics can change soil properties and affect plant performance. Environ Sci Technol. 2019;53(10):6044–52. https://doi.org/10.1021/acs.est.9b01339.
21. Rillig MC, Lehmann A. Microplastic in terrestrial ecosystems. Science. 2020;368(6498):1430–1. https://doi.org/10.1126/science.abb5979.
22. Rillig MC, Lehmann A, Souza Machado AA, Yang G. Microplastic effects on plants. New Phytol. 2019;223(3):1066–70. https://doi.org/10.1111/nph.15794.
23. Woodford L, Fellows R, White HL, Ormsby MJ, Pow CJ, Quilliam RS. Survival and transfer potential of *Salmonella enterica* serovar Typhimurium colonising polyethylene microplastics in contaminated agricultural soils. Environ Sci Pollut Res. 2024. https://doi.org/10.1007/s11356-024-34491-4.
24. Liu M, Lu S, Chen Y, Cao C, Bigalke M, He D. Analytical Methods for Microplastics in Environments: Current Advantages and Challenges. In: He D, Luo Y, Barceló D, Kostianoy AG, editors. Microplastics in Terrestrial Environments. Emerging Contaminants and Major Challenges. The

Handbook of Environmental Chemistry, vol. 95. Springer Nature Switzerland AG; 2021.
25. Dorau K, Hoppe M, Rückamp D, Köser J, Scheeder G, Scholz K, et al. Status quo of operation procedures for soil sampling to analyze microplastics. Microplastics Nanoplastics. 2023;3(1): 15. https://doi.org/10.1186/s43591-023-00063-5.
26. Weber CJ, Opp C. Spatial patterns of mesoplastics and coarse microplastics in floodplain soils as resulting from land use and fluvial processes. Environ Pollut. 2020;267: 115390. https://doi.org/10.1016/j.envpol.2020.115390.
27. Kelletat AS, Jimenez-Martinez J, Mitrano DM. Transport of nano-and microplastic through unsaturated porous media from sewage sludge application. Environ Sci Technol. 2019;54:911–20. https://doi.org/10.1021/acs.est.9b06483.
28. Brandes E, Braun M, Rillig MC, Leifheit EF, Steinmetz Z, Fiener P, et al. (Mikro-)Plastik im Boden. Bodenschutz. 2020;3/2020:121–125. https://doi.org/10.37307/j.1868-7741.2020.03.10.
29. Huerta Lwanga E, Gertsen H, Gooren H, Peters P, Salánki T, van der Ploeg M, et al. Incorporation of microplastics from litter into burrows of *Lumbricus terrestris*. Environ Pollut. 2017;220:523–31. https://doi.org/10.1016/j.envpol.2016.09.096.
30. Engdahl NB. Simulating the mobility of micro-plastics and other fiber-like objects in saturated porous media using constrained random walks. Adv Water Resour. 2018;121:277–84.
31. Gao J, Pan S, Li P, Wang L, Hou R, Wu WM, et al. Vertical migration of microplastics in porous media: multiple controlling factors under wet-dry cycling. J Hazard Mater. 2021;419: 126413. https://doi.org/10.1016/j.jhazmat.2021.126413.
32. Heinze WM, Steinmetz Z, Klemmensen NDR, Vollertsen J, Cornelis G. Vertical distribution of microplastics in an agricultural soil after long-term treatment with sewage sludge and mineral fertiliser. Environ Pollut. 2024;356: 124343. https://doi.org/10.1016/j.envpol.2024.124343.
33. O'Connor D, Pan S, Shen Z, Song Y, Jin Y, Wu WM, et al. Microplastics undergo accelerated vertical migration in sand soil due to small size and wet-dry cycles. Environ Pollut. 2019;249:527–34. https://doi.org/10.1016/j.envpol.2019.03.092.
34. Gu J, Chen L, Wan Y, Teng Y, Yan S, Hu L. Experimental investigation of water-retaining and unsaturated infiltration characteristics of loess soils imbued with microplastics. Sustainability. 2022;15(1):62. https://doi.org/10.3390/su15010062.
35. Tong M, He L, Rong H, Li M, Kim H. Transport behaviors of plastic particles in saturated quartz sand without and with biochar/Fe3O4-biochar amendment. Water Res. 2020;169: 115284. https://doi.org/10.1016/j.watres.2019.115284.
36. Qi S, Song J, Shentu J, Chen Q, Lin K. Attachment and detachment of large microplastics in saturated porous media and its influencing factors. Chemosphere. 2022;305:135322. https://doi.org/10.1016/j.chemosphere.2022.135322.
37. Park S, Kim I, Jeon WH, Moon HS. Exploring the vertical transport of microplastics in subsurface environments: lab-scale experiments and field evidence. J Contam Hydrol. 2023;257: 104215. https://doi.org/10.1016/j.jconhyd.2023.104215.
38. Yu Y, Flury M. Current understanding of subsurface transport of micro- and nanoplastics in soil. Vadose Zone J. 2021; e20108. https://doi.org/10.1002/vzj2.20108.
39. Deutscher Wetterdienst. Klimadiagramm von Köln/Bonn (Flugh.), Nordrhein-Westfalen / Deutschland. 2022. https://www.dwd.de/DWD/klima/beratung/ak/ak_105130_di.pdf. Accessed 3 July 2023.
40. Geologischer Dienst Nordrhein-Westfalen. IS BK 50 Bodenkarte. 2023. https://www.geoportal.nrw/. Accessed 19 Jan 2023.
41. Information und Technik Nordrhein-Westfalen. ELWAS-WEB, Grundwassermessstellen. Ministerium für Umwelt, Naturschutz und Verkehr des Landes NordrheinWestfalen; 2023. https://www.elwasweb.nrw.de/. Accessed 8 Feb 2023.
42. Brasseur GP, Jacob D, Schuck-Zöller S, editors. Klimawandel in Deutschland. Berlin, Heidelberg: Springer Berlin Heidelberg; 2017. https://doi.org/10.1007/978-3-662-50397-3.
43. Krapesch M, Klösch M, Ten Brinke W, Habersack H. The rhine catchment: a review of sediment-related knowledge, monitoring, and a future research perspective. Water. 2024;16(8): 1121. https://doi.org/10.3390/w16081121.
44. QGIS Development Team. QGIS Geographic Information System. QGIS Association; 2023. https://www.qgis.org.
45. FAO. Guidelines for soil description. 4th ed. Rome: Food and Agriculture Organization of the United Nations; 2006. OCLC: ocm71825863.
46. FAO. World reference base for soil resources 2014: international soil classification system for naming soils and creating legends for soil maps. Rome: FAO; 2014. OCLC: 979061096.
47. Murray AS, Wintle AG. The single aliquot regenerative dose protocol: potential for improvements in reliability. Radiat Meas. 2003;37(4–5):377–81. https://doi.org/10.1016/S1350-4487(03)00053-2.
48. Arnold LJ, Roberts RG. Stochastic modelling of multi-grain equivalent dose (De) distributions: implications for OSL dating of sediment mixtures. Quat Geochronol. 2009;4(3):204–30. https://doi.org/10.1016/j.quageo.2008.12.001.
49. Ju H, Yang X, Osman R, Geissen V. Effects of microplastics and chlorpyrifos on earthworms (*Lumbricus terrestris*) and their biogenic transport in sandy soil. Environ Pollut. 2023;316: 120483. https://doi.org/10.1016/j.envpol.2022.120483.
50. Rillig MC, Ziersch L, Hempel S. Microplastic transport in soil by earthworms. Sci Rep. 2017;7(1): 1362. https://doi.org/10.1038/s41598-017-01594-7.
51. Sims RW, Gerard RM. Earthworms: Keys and Notes for the Identification and Study of the Species. Synopses of the British fauna (New series), vol. 31. Shrewsbury: Field studies council; 1999.
52. Bouché MB. Strategies lombriciennes Ecol Bull. 1977;25:122–32.
53. Krück S. Bildatlas zur Regenwurmbestimmung mit einem Kompendium der Regenwurmfauna des Nordostdeutschen Tieflandes. Natur+Text; 2018.
54. Möller JN, Heisel I, Satzger A, Vizsolyi EC, Oster J, Agarwal S, et al. Tackling the challenge of extracting microplastics from soils: a protocol to purify soil samples for spectroscopic analysis. Environ Toxicol Chem. 2021;41:844–57. https://doi.org/10.1002/etc.5024.
55. Deutsches Institut für Normung e V . DIN EN 15934:2012-11, Schlamm, behandelter Bioabfall, Boden und Abfall – Berechnung des Trockenmasseanteils nach Bestimmung des Trockenrückstands oder des Wassergehalts. Beuth-Verlag; 2012. https://doi.org/10.31030/1866718.
56. Löder MGJ, Imhof HK, Ladehoff M, Löschel LA, Lorenz C, Mintenig S, et al. Enzymatic purification of microplastics in environmental samples. Environ Sci Technol. 2017;51(24):14283–92. https://doi.org/10.1021/acs.est.7b03055.
57. Hufnagl B, Stibi M, Martirosyan H, Wilczek U, Möller JN, Löder MGJ, et al. Computer-assisted analysis of microplastics in environmental samples based on µFTIR imaging in combination with machine learning. Environ Sci Technol Lett. 2022;9(1):90–5. https://doi.org/10.1021/acs.estlett.1c00851.
58. Kiene M, Vizsolyi Cseperke E, Löder M, Laforsch C. evalPurency: Automated Evaluation of Data of the Purency's Microplastic Finder. 2023. https://github.com/Maki-science/evalPurency. (Accessed on 13.02.2023)
59. RStudio Team. RStudio: Integrated Development for R. Boston: RStudio, PBC; 2020. http://www.rstudio.com/.
60. R Core Team. R: a language and environment for statistical computing. Vienna: R Foundation for Statistical Computing; 2022.
61. Wickham H, Averick M, Bryan J, Chang W, McGowan L, François R, et al. Welcome to the tidyverse. J Open Source Softw. 2019;4(43): 1686.
62. Frings RM, Hillebrand G, Gehres N, Banhold K, Schriever S, Hoffmann T. From source to mouth: basin-scale morphodynamics of the Rhine River. Earth Sci Rev. 2019;196: 102830. https://doi.org/10.1016/j.earscirev.2019.04.002.
63. Fliegel G, Krause PG, Quaas A, Wunstorf W, Zimmermann E. Geologische Karte von Preußen und benachbarten deutschen Ländern, Blatt 4907 "Leverkusen". Berlin: Preußische Geologische Landesanstalt; 1927.
64. Amelung W, Blume HP, Fleige H, Horn R, Kandeler E, Kögel-Knabner I. Scheffer/schachtschabel lehrbuch der bodenkunde. Berlin, Heidelberg: Springer Berlin Heidelberg; 2018. https://doi.org/10.1007/978-3-662-55871-3.

65. Shipitalo MJ, Le Bayon RC. Quantifying the effects of earthworms on soil aggregation and porosity. Earthworm Ecology. 2nd ed. 2004. pp. 183–200. https://doi.org/10.1201/9781420039719.pt5.
66. van Schaik L, Palm J, Klaus J, Zehe E, Schröder B. Linking spatial earthworm distribution to macropore numbers and hydrological effectiveness. Ecohydrol. 2013;7(2):401–8. https://doi.org/10.1002/eco.1358.
67. Jiao J, Chen G, Yang Z, Li Z, Hu H. Microplastics in Surface Waters and Floodplain Sediments of the Dagu River in the Jiaodong Peninsula. China J Ocean Univ China. 2022;21(6):1538–48. https://doi.org/10.1007/s11802-022-5211-z.
68. Hurley RR, Nizzetto L. Fate and occurrence of micro(nano)plastics in soils: knowledge gaps and possible risks. Curr Opin Environ Sci Health. 2018;1:6–11. https://doi.org/10.1016/j.coesh.2017.10.006.
69. Cao L, Wu D, Liu P, Hu W, Xu L, Sun Y, et al. Occurrence, distribution and affecting factors of microplastics in agricultural soils along the lower reaches of Yangtze River. China Sci Total Environ. 2021;794:148694. https://doi.org/10.1016/j.scitotenv.2021.148694.
70. Christensen ND, Wisinger CE, Maynard LA, Chauhan N, Schubert JT, Czuba JA, et al. Transport and characterization of microplastics in inland waterways. J Water Process Eng. 2020;38: 101640. https://doi.org/10.1016/j.jwpe.2020.101640.
71. Yuan B, Gan W, Sun J, Lin B, Chen Z. Depth profiles of microplastics in sediments from inland water to coast and their influential factors. Sci Total Environ. 2023. https://doi.org/10.1016/j.scitotenv.2023.166151.
72. Dimante-Deimantovica I, Saarni S, Barone M, Buhhalko N, Stivrins N, Suhareva N, et al. Downward migrating microplastics in lake sediments are a tricky indicator for the onset of the Anthropocene. Sci Adv. 2024;10(8):eadi8136. https://doi.org/10.1126/sciadv.adi8136.
73. Zhou Y, Liu X, Wang J. Characterization of microplastics and the association of heavy metals with microplastics in suburban soil of central China. Sci Total Environ. 2019;694: 133798. https://doi.org/10.1016/j.scitotenv.2019.133798.
74. Mani T, Hauk A, Walter U, Burkhardt-Holm P. Microplastics profile along the Rhine River. Sci Rep. 2015;5(1): 17988. https://doi.org/10.1038/srep17988.
75. Plastics Europe AISBL. Plastics – the Facts 2022. 2022. https://plasticseurope.org/wp-content/uploads/2022/12/PE-PLASTICS-THE-FACTS_FINAL_DIGITAL.pdf. Accessed 18 Feb 2023.
76. Waldschläger K, Schüttrumpf H. Infiltration behavior of microplastic particles with different densities, sizes, and shapes-from glass spheres to natural sediments. Environ Sci Technol. 2020;54(15):9366–73. https://doi.org/10.1021/acs.est.0c01722.
77. Huerta Lwanga E, Gertsen H, Gooren H, Peters P, Salánki T, van der Ploeg M, et al. Microplastics in the terrestrial ecosystem: implications for *Lumbricus terrestris* (Oligochaeta, Lumbricidae). Environ Sci Technol. 2016;50(5):2685–91. https://doi.org/10.1021/acs.est.5b05478.
78. Holzinger A, Hink L, Sehl E, Rüppel N, Lehndorff E, Weig AR, et al. Biodegradable polymers boost reproduction in the earthworm *Eisenia fetida*. Sci Total Environ. 2023;892: 164670. https://doi.org/10.1016/j.scitotenv.2023.164670.
79. Bartlett MD, Briones MJI, Neilson R, Schmidt O, Spurgeon D, Creamer RE. A critical review of current methods in earthworm ecology: from individuals to populations. Eur J Soil Biol. 2010;46(2):67–73. https://doi.org/10.1016/j.ejsobi.2009.11.006.
80. Gutiérrez-López M, Moreno G, Trigo D, Juárez E, Jesús JB, Díaz Cosín DJ. The efficiency of earthworm extraction methods is determined by species and soil properties in the Mediterranean communities of central-western Spain. Eur J Soil Biol. 2016;73:59–68. https://doi.org/10.1016/j.ejsobi.2016.01.005.
81. Rehm R, Zeyer T, Schmidt A, Fiener P. Soil erosion as transport pathway of microplastic from agriculture soils to aquatic ecosystems. Sci Total Environ. 2021;795: 148774. https://doi.org/10.1016/j.scitotenv.2021.148774.
82. Li W, Brunetti G, Bolshakova A, Stumpp C. Effect of particle density on microplastics transport in artificial and natural porous media. Sci Total Environ. 2024;935: 173429. https://doi.org/10.1016/j.scitotenv.2024.173429.
83. Yang X, Tang DWS. Modeling microplastic transport through porous media: challenges arising from dynamic transport behavior. J Hazard Mater. 2025;484: 136728. https://doi.org/10.1016/j.jhazmat.2024.136728.
84. Stauch G, Schulte P, Schwanen C, Kümmerle EA, Dörwald L, Esch A, et al. 115 years of sediment deposition in a reservoir in Central Europe: effects of the industrial history and environmental protection on heavy metals and microplastic. Earth Surf Process Landforms. 2024; 5914. https://doi.org/10.1002/esp.5914.
85. Hallam J, Hodson ME. Impact of different earthworm ecotypes on water stable aggregates and soil water holding capacity. Biol Fertil Soils. 2020;56(5):607–17. https://doi.org/10.1007/s00374-020-01432-5.
86. Capowiez Y, Bottinelli N, Sammartino S, Michel E, Jouquet P. Morphological and functional characterisation of the burrow systems of six earthworm species (Lumbricidae). Biol Fertil Soils. 2015;51(7):869–77. https://doi.org/10.1007/s00374-015-1036-x.
87. Le Mer G, Jouquet P, Capowiez Y, Maeght J, Tran TM, Doan TT, et al. Age matters: dynamics of earthworm casts and burrows produced by the anecic *Amynthas khami* and their effects on soil water infiltration. Geoderma. 2021;382: 114709. https://doi.org/10.1016/j.geoderma.2020.114709.
88. Zalasiewicz J, Waters CN, Ivar do Sul JA, Corcoran PL, Barnosky AD, Cearreta A, et al. The geological cycle of plastics and their use as a stratigraphic indicator of the anthropocene. Anthropocene. 2016;13:4–17. https://doi.org/10.1016/j.ancene.2016.01.002.
89. Weber CJ, Lechthaler S. Plastics as a stratigraphic marker in fluvial deposits. Anthropocene. 2021;36: 100314. https://doi.org/10.1016/j.ancene.2021.100314.

Publisher's Note